ELSEVIER

Physica B 297 (2001) 1–8

PHYSICA B

www.elsevier.com/locate/physb

# Neutron beams at the spin revolution

F. Tasset*

*Science Division, Institut Laue–Langevin, B.P. 156, 38042 Grenoble Cedex 9, France*

**Abstract**

Spherical neutron polarimetry (SNP), as implemented at ILL with the second-generation zero-field polarimeter CRYOPAD II, enables to orient precisely the spin polarisation vector in the incident thermal neutron beam and to measure how it is changed (amplitude and direction) by interaction with the sample. For neutrons scattered by excitations in low-dimension magnetic systems, the components which are transverse to the initial polarisation direction are large and could be recently and systematically observed by Regnault et al. (Physica B 267–268 (1999) 227.). Maleyev has shown that such transverse components can arise uniquely from the existence of mixed nuclear-magnetic Van–Hove pair correlation functions. Therefore, neutron scattering is telling us that the excitations are strongly hybridized. We discuss what are the most important technical features of this ultimate polarised neutron technique in view of this fascinating application of inelastic neutron scattering for the years to come. © 2001 Elsevier Science B.V. All rights reserved.

*Keywords:* Neutron polarimetry; Cryopad, Nuclear-magnetic interference terms

## 1. Introduction

It has been said that the coming decades are the decades of phase coherence in solid-state physics. Fifty years after the transistor was invented, we are getting close to the point where a single-electron spin will hopefully be used to record a bit of information. In that context, solid-state physicists are urged to identify which interactions are to be incorporated in a theory to properly predict how electron spins can be stored and transported in an appropriate condensed media. The interplay in between spin and lattice degrees of freedom will obviously play a very important role in this forthcoming development. It will be necessary to go from a thermodynamic (entropic) view for the uncontrolled degrees of freedom to a more deterministic, albeit quantum mechanical, view. We shall assist to a complete rebirth of solid-state physics into a solid-state engineering science where many important effects will appear, due to the electron spin state being coherent over such typical nanometer size objects. Computer simulation will be essential to conceive such advanced tools, but nothing will finally work if we do not understand in depth the tiny, low-energy mechanisms which regulate spin transportation. As usual, spectroscopy will play an important role by setting the scene in time and elastic scattering the scene in space variables. But in order to regulate time, space and spin variables together, that is organize spin-polarized

* Fax: + 33-4-76-20-76-48.
*E-mail address:* francis.tasset@ill.fr (F. Tasset).


PII: S0921-4526(00)00874-7

traffic, a fully coherent picture is certainly needed. The object of this paper is to suggest with a couple of example that the neutron and its coherent dual scattering at magnetic induction fields and the underlying atomic lattice, might well be uniquely gifted to properly set the emerging conceptual scene of Spintronics.

## 2. Polarimetric neutron scattering

The neutron is a point particle, which is carrying its own spin angular momentum. Being a measurable quantity, the spin angular momentum has three components, which transform in each other like the D1 irreducible representation of the rotation group. In simpler words, it is a classical 3d vector. In the absence of external interaction, the angular momentum conservation law applies and the spin is indefinitely conserved parallel to itself. But, attached to this spin-angular momentum, the neutron carries a magnetic moment, which makes it interact with magnetic induction fields. Therefore, measuring the rotation of the neutron spin vector is a powerful way to investigate the magnetic field that it has been crossing during its life.

This can be used to investigate field integrals in macroscopic magnetic cavities (Larmor coils, zero-field cavities), magnetic domains in magnets and recording media, and ultimately at atomic size to investigate magnetic order and atomic magnetization densities. Imagine for a second that you extract a very dense and monochromatic beam of neutron from a neutron star. Due to some nuclear interactions in this extremely dense source the beam is magnetized. You can see that easily by just turning a Hall probe in the beam. It becomes a trivial measurement to see how the spin polarization rotates when crossing your sample. Measuring the rotation of the neutron spin in presently available neutron beams is not so easy but it can be done. One has to use spin filters and neutron detectors. This is the way the incident beam is magnetized and the final direction of magnetization is measured.

The spin of the neutron is $\frac{1}{2}$, that is to say its angular momentum is $\frac{1}{2}\hbar$, the smallest possible one. Because the neutron angular momentum is very small, the individual neutron counting measurement has to be handled quantum mechanically. Measuring a component of it is a fully quantized process where the single neutron being looked at appears as having only two possible eigenstates with eigenvalues values for the spin component $(\pm\frac{1}{2})\hbar$. Therefore, measuring the beam magnetization in that direction requires to observe many neutrons and to calculate $(n^+ - n^-)/(n^+ + n^-)$ and the standard deviation on this quantity. When you are satisfied with this measurement you might like to measure a second component of the vector and a third one. Note that it is only when you find zero for the three measurements that you can safely say that the beam is unpolarized.

It is quite instructive to demonstrate, starting from the time-dependent quantum mechanical equation in a magnetic induction field, that the expectation values of the beam magnetization vector obey the same Larmor equation as in classical mechanics. This has been extremely useful for the conception of many neutron polarization tools like Larmor coils. But one should not forget that this would not stay true as soon as the magnetic field inhomogeneities become comparable to the neutron wavelength. Then scattering and diffraction effects have to be taken into account fully using the Schrödinger equation. This is the domain of polarimetric neutron scattering.

### 2.1. *Principle of the polarimetric neutron scattering experiment* (*Fig. 1*)

### 2.2. *Theory of polarimetric neutron scattering*

#### 2.2.1. *The nuclear structure factor and the magnetic interaction vector*

Let us call $F_N(\boldsymbol{Q})$[cm] the nuclear structure factor and $\boldsymbol{F}_M(\boldsymbol{Q})[\mu_B]$ the vectorial magnetic structure factor, $\boldsymbol{Q}$ being the scattering vector. In a magnetic crystal, the magnetic moment of the neutron interacts with the periodic field of the magnetic electrons resulting in magnetic scattering amplitude. Due to the dipolar nature of this coupling only the component of $\boldsymbol{F}_M(\boldsymbol{Q})$ which is perpendicular to $\boldsymbol{Q}$ is effective.

$$\boldsymbol{F}_{M\perp}(Q) = \hat{Q} \wedge (\boldsymbol{F}_M(\hat{Q}) \wedge \hat{Q}). \quad (1)$$

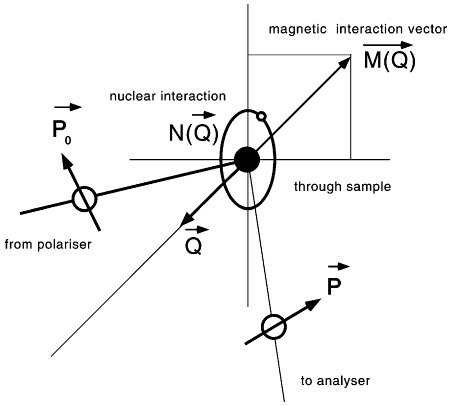


Fig. 1. Principle of Neutron Polarimetry. The incident polarized beam is scattered at wave vector $Q$. The incident polarization vector is oriented in a particular direction. Due to the magnetic interaction, it rotates in a way which tells us about the $Q$ Fourier components of the magnetic and nuclear potential experienced in the sample.

It can be shown that the corresponding neutron scattering amplitude operator, expressed in the spin space of the neutron, reads:

$$a_{\mathrm{M}}(\boldsymbol{Q}) = p\boldsymbol{F}_{\mathrm{M}\perp}(\boldsymbol{Q})\cdot\boldsymbol{\sigma}. \quad (2)$$

The vector operator $\boldsymbol{\sigma}$ has three components, which are the Pauli matrices and

$$p = 0.2695\times10^{-12}\ [\mathrm{cm}/\mu_{\mathrm{B}}] \quad (3)$$

is the scattering length corresponding to one Bohr magneton.

It is then useful to define the magnetic interaction vector: $\boldsymbol{M}(\boldsymbol{Q}) = p\boldsymbol{F}_{\mathrm{M}\perp}(\boldsymbol{Q})$ which is represented in Fig. 2.

*2.2.2. The master equations for neutron polarimetry*

Using the density matrix formalism, within Born approximation, Blume [1] and Maleyev et al. [2] could predict the scattering cross-section and the scattered polarization vector in the most general case. In Table 1, the two master SNP equations are physically splitted into four different parts.

## 2.3. Experimental techniques

*2.3.1. LPA: limitations due to the application of a guide field*

Following early experiments at Gatchina [16], an arrangement was built at Oak Ridge [3] to look

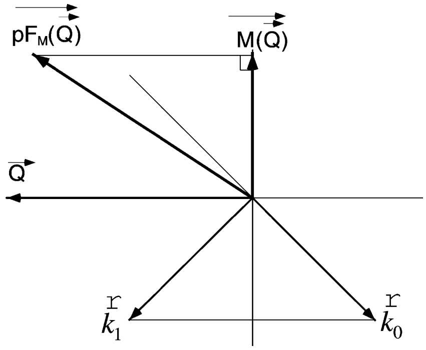


Fig. 2. The magnetic interaction vector.

systematically at the scattered neutron polarisation outside the direct beam. The direction of the incident polarization vector $\boldsymbol{P}_0$ was set adiabatically in an arbitrary direction using a strong enough magnetic guide-field at the sample position. This particular axis was called $z$ and, in the absence of any further coil arrangement, it was recognized that not the whole scattered polarization $\boldsymbol{P}$ (see Fig. 3) could be analyzed, only the "longitudinal component" $P_z$. This was clearly due to the fact that the final spin analyzer was only sensitive to this particular component. (In addition the transverse component which starts precessing quickly in the field is very difficult to measure.)

Moon, Riste and Koehler [3] (MRK), being convinced that it was impossible to achieve polarization analysis without the help of a guide field, focussed all their attention on $P_z$. In a simplified theory they produced a subset of 4-spin-state indexed cross-sections which became famous:

$$\sigma_{zz}^{++} = |\langle b + pS_{\perp}^{z}\rangle|^2,$$

$$\sigma_{zz}^{--} = |\langle b - pS_{\perp}^{z}\rangle|^2,$$

$$\sigma_{zz}^{+-} = |\langle p\cdot S_{\perp}^{x} + \mathrm{i}S_{\perp}^{y}\rangle|^2,$$

$$\sigma_{zz}^{-+} = |\langle p\cdot S_{\perp}^{x} - \mathrm{i}S_{\perp}^{y}\rangle|^2.$$

We have added as a subscript to the partial $\sigma$'s the 2-axis of quantification $zz$ (pre- and post-scattering) which were implicit in MRK mind but unfortunately forgiven in their notations. Although it would have been possible to extract the expressions for the cross-sections from the completely general Blume's equations already published, MRK deliberately

Table 1
The four main parts in elastic polarimetric neutron scattering[a]

| (Index)/mode | Elastic contribution | Comment |
|---|---|---|
| (n) Nuclear | $\sigma_n = NN^*$<br>$(\boldsymbol{P\sigma})_n = \boldsymbol{P}_0\sigma_n$ | Intensity as modulus square of the structure factor<br>Incident Polarization is conserved |
| (m) Magnetic normal part | $\sigma_m = \boldsymbol{M}\cdot\boldsymbol{M}^*$<br>$(\boldsymbol{P\sigma})_m = -\boldsymbol{P}_0\sigma_m\{1-2(\hat{P}_0\cdot\hat{M})\hat{M}\}$ | Intensity as modulus square of the magnetic interaction vector (MIV)<br>Incident Polarization is flipped except for its component along the MIV |
| (c) Magnetic chiral part | $\sigma_c = i(\boldsymbol{M}^*\times\boldsymbol{M})\cdot\boldsymbol{P}_0$<br>$(\boldsymbol{P\sigma})_c = -i(\boldsymbol{M}^*\times\boldsymbol{M})$ | Intensity depends on incident Polarization.<br>$\boldsymbol{M}\times\boldsymbol{M}^*\neq 0$ creates Polarization along the scattering vector |
| (i) Nuclear-mag. Interference | $\sigma_i = (N\boldsymbol{M}^* + N^*\boldsymbol{M})\cdot\boldsymbol{P}_0$<br>$(\boldsymbol{P\sigma})_i = N\boldsymbol{M}^* + N^*\boldsymbol{M} - i[(N\boldsymbol{M}^* - N^*\boldsymbol{M})\times\boldsymbol{P}_0]$ | Intensity depends on incident polarization when N&M are in phase<br>Polarization is created along $\boldsymbol{M}$ when N&M are in phase. Incident polarization is rotated on a cone around $\boldsymbol{M}$ when N&M are in quadrature. |

[a] $\sigma_t = \sigma_n + \sigma_m + \sigma_c + \sigma_i$;  $\boldsymbol{P}\sigma_t = (\boldsymbol{P\sigma})_n + (\boldsymbol{P\sigma})_m + (\boldsymbol{P\sigma})_c + (\boldsymbol{P\sigma})_i$.

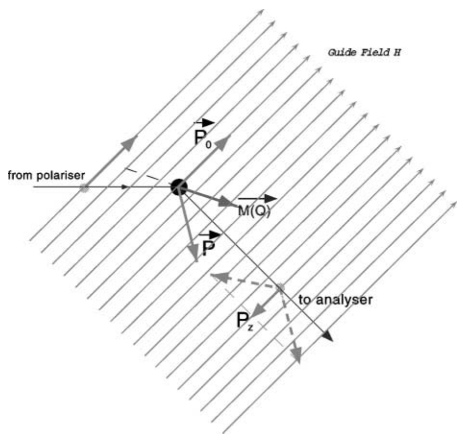


Fig. 3. Longitudinal polarization analysis [LPA]: Measuring the "Longitudinal component" of scattered polarization $P_z$ in a guide-field.

lost any explicit mention to the transverse components in their presentation. LPA having been the only technique available at finite $\boldsymbol{Q}$ for 20 years, experimentalist got used to the MRK presentation, forgetting that they were not necessarily measuring the final polarization, just a particular component of it. This is illustrated by the almost universal, albeit improper name, "Full Polarization Analysis" used for the MRK arrangement. When using the zero-field Cryopad arrangement we have access to 12 independent cross-sections ($\sigma_{zz}^{++}$, $\sigma_{zz}^{--}$, $\sigma_{zz}^{+-}$, $\sigma_{zz}^{-+}$, $\sigma_{zx}^{++}$, $\sigma_{zx}^{--}$, $\sigma_{zx}^{+-}$, $\sigma_{zx}^{-+}$, $\sigma_{zy}^{++}$, $\sigma_{zy}^{--}$, $\sigma_{zy}^{+-}$, $\sigma_{zy}^{-+}$) and we use "longitudinal polarization analysis" (LPA) to describe the MRK subset of measurements. One should always be cautious with too strong an interpretation of the LPA results: because LPA is unable to detect the transverse component of polarization, it is not possible to distinguish a true depolarization effect from a "trivial" rotation of the polarization vector. SNP has no such drawback and should be preferred in all antiferromagnetic studies where the application of a magnetic field at the sample position is not strictly required.

### 2.3.2. *SNP: the zero-field chamber approach*

For a long time, the theory of General Polarization Analysis [1] had established that the measurement of all the three components of the final polarization were interesting, being sometimes the only means to decide in between two magnetic configurations. [4]. Such a measurement is a difficult experimental task knowing the strong influence of any magnetic field on neutron polarization. In fact, it requires connecting two different guide-field directions onto a zero-field sample chamber. Alperin demonstrated this in a pioneering experiment where he could show the existence of very large transverse components of polarization in a low-angle reflection on a $Cr_2O_3$ crystal [4].

### 2.3.3. *Cryopad: implementing SNP at arbitrary momentum transfer*

Following Rekveldt [5] and Okorokov [6], who had built early zero-field polarimeters which were successfully used for transmission and SANS measurements, we have been able to extend the accessible $Q$ range in a radical way by building the wall of the zero-field sample chamber with a cryocooled Nb cylinder (Fig. 4). Niobium is quite transparent to neutrons, let the neutron polarization vector be unchanged and at the same time provide an extremely effective diamagnetic shield across the beam.

Therefore, Cryopad is able to achieve full vectorial control of neutron polarization at high $Q$ in order to exploit fully the theory shown in the preceding section. Receiving a polarized monochromatic beam from a primary spectrometer, Cryopad orients the polarization vector in any specific direction and then delivers it to the sample chamber. The sample chamber is maintained in a zero-field state, there is no parasitic precession and the change in polarization, therefore, results only from

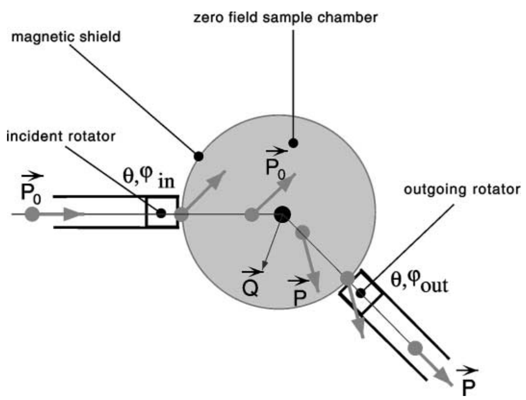


Fig. 4. Spherical neutron polarimetry [SNP]: Measuring all 3 components of scattered polarization in zero-field.

the interactions present in the scattering process. When the final polarization vector exits from the sample chamber, Cryopad acts on it in order to deliver one by one each three components in turn to the analyzer. More details on the design of this polarimeter and the technique of generalized polarization analysis can be found in Refs. [7–9].

### 2.3.4. *Cryopadum: going forward with Cryopad by combining Mu-metal and Meissner shields*

In Cryopad-I the precession angles were controlled with small vertical coils, one being moved inside the cryostat in order to intercept the scattered beam. In Cryopad-II, a monolithic system based on a superposition of two horizontal superposed toroidal coils was developed. This second system was a nice step forward [10]. It turns to be very practical and giving satisfaction to within 2° of absolute precision when intercepting an incoming beam less than 2 cm in diameter. Due to the current IN20 development toward larger divergence for the incoming beam there is a need to increase the size of the homogeneous region in the Larmor coil intercepting the incident beam. According to recent computer simulations by M. Thomas, it is possible to achieve a high homogeneity in compact coils by combining Meissner shields and Mu-metal yokes in their construction. This new design will also remove the systematic errors due to the superposition of the primary and secondary fields present in the design of Cryopad-II. Finally, a better external mu-shield will be built to improve the zero-field condition in the sample chamber. That way, we expect a significant improvement in the built- in absolute precision of this new version. Limitations due to wavelength spread might well become the limiting factor for Cryopadum in elastic mode.

## 3. Exploiting the interference terms

### 3.1. *The high-Q part of the antiferromagnetic Cr form factor in $Cr_2O_3$ as obtained with short wavelength and the $^3He$ spin filter [11]*

$Cr_2O_3$ provides a well-known example of an antiferromagnet for which magnetic and nuclear

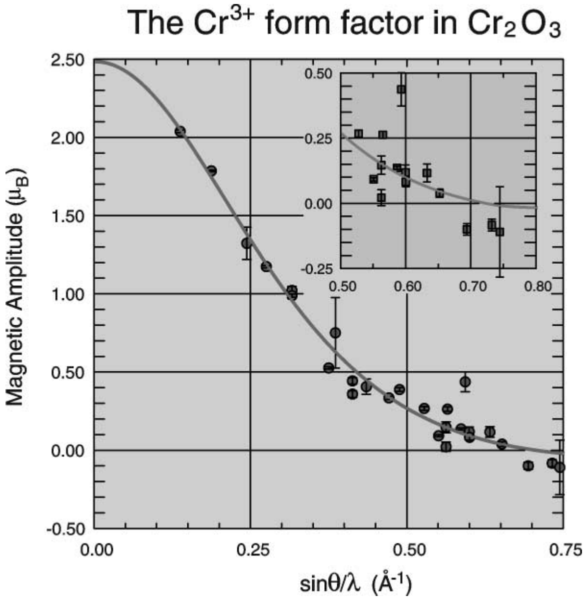


Fig. 5. The magnetic form factor measured at the $h0.\ell$ Bragg reflections of $Cr_2O_3$. The smooth curve is the spin-only free ion form factor for $Cr^{3+}$ normalized to $2.5\mu_B$.

scattering appear in the same Bragg reflections and are in phase quadrature.

We have already measured the ratios of all reflections of the form $h0.\ell$ with $\sin\theta/\lambda < 0.5$ Å$^{-1}$ using Cryopad II on IN20 [12]. These measurements, which were made on two crystals of different sizes in three different degrees of domain imbalance, gave amazingly consistent results which enabled the lower-angle part of the $Cr^{3+}$ form factor shown in Fig. 5 to be determined with high precision. It is not however possible to extend these measurements to higher $\sin\theta/\lambda$ using IN20 since the highest useable incident wave vector is 4.1/1 Å$^{-1}$.

However, we have recently been able to extend our measurements to higher-momentum transfer by installing Cryopad on the hot-source-polarized neutron diffractometer D3 and using the newly available $^3$He-neutron spin filter [13] to allow polarization analysis of the diffracted beam. At the higher $\sin\theta/\lambda$ values the magnetic scattering becomes very weak and it is impractical to carry out the full polarization analysis. However, if the domain ratio is high and is determined using the lower-angle reflections, then it is sufficient to measure just $P_{xz}$ and $P_{zx}$ components of scattered polarization. These are linearly rather than quadratically dependent on the magnetic amplitudes and may be corrected for deficiencies in the transmitted polarization using the $P_{yy}$ component. Using this method, we are able to deduce the magnetic structure factors of 14 $h0.\ell$ reflections with $\sin\theta/\lambda$ between 0.5 and 0.75 Å$^{-1}$. Their contributions to the $Cr^{2+}$ form factor are shown in Fig. 5 and are magnified in the inset.

We were able to fit the low-angle data to the $Cr^{3+}$ free atom form factor by assuming a chromium moment of $2.5\mu_B$. The rather low value suggests that there is significant covalent transfer to the oxygen ligands. These lower-angle data fit rather well onto a smooth curve. The higher-angle data are scattered above and below the curve corresponding to a spherical distribution of moment, this scatter contains information about the deviations from spherical symmetry and can be used to determine the distribution of unpaired electrons amongst the different 3d orbitals.

### 3.2. The $CuGeO_3$ hybrid excitations [14]

Results obtained on the low-energy excitation spectrum of the inorganic spin-Peierls compound $CuGeO_3$ by using inelastic neutron polarimetry are quite exciting. A sizable rotation of the neutron polarization $\boldsymbol{P}$ is observed in the $b, c$ plane when the incident polarization $\boldsymbol{P}_0$ is set parallel or perpendicular to the scattering vector $\boldsymbol{Q}$ in the horizontal plane (see Fig. 6).

The qualitative analysis of the $\boldsymbol{P}_0$ and $\boldsymbol{Q}$-dependencies on the three components of $\boldsymbol{P}$ leads us to ascribe this rotation to an effect of the inelastic nuclear-magnetic interference terms. These findings can be qualitatively understood by considering the elementary excitations in $CuGeO_3$ as composite objects mixing the magnetic and structural degrees of freedom. The strong transverse components of scattered polarization might originate from the existence in the vicinity of the oxygen-O(2) sites of a dynamical magnetization density mainly polarized along the $a$-axis, very likely of orbital origin.

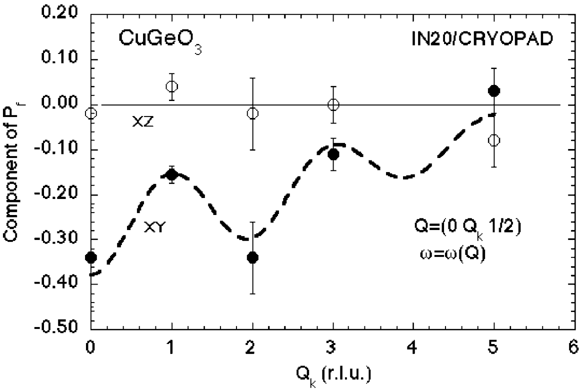


Fig. 6. The $Q$ dependance of the large transverse component of polarisation found in $CuGeO_3$.

## 4. Conclusion

For people interested in only one science, crystallography or magnetism, the fact that the neutron scatters both on nuclei and magnetic electrons appears as a complication. This is why the neutron-spin polarization is often considered as an adhoc means to switch the magnetic scattering in view of "separating" the two contributions when they both exist.

In the field of static atomic and molecular magnetism the spin-dependent nuclear-magnetic interference term contained in the neutron cross-section allows us, since a long time, to measure very small magnetic amplitude by reversing the incident neutron polarization. This very sensitive technique, the flipping ratio measurement [FR] has been successfully used in the past for the determination of "ferromagnetic" atomic form factor, giving the exact shape and spatial density of magnetic ions aligned in a field. For $k = 0$ antiferromagnetic arrangements (as in magneto-electric compounds), where the cross-section does not depend on incident polarization the FR technique fails, leaving room for a superb extension which recently emerged from the observation of the transverse component of polarization using our novel SNP method.

But the exciting application of polarimetric neutron scattering is in the inelastic mode. On the one hand, the concept of mixed spin-lattice excitations is playing a growing role in discussions on high-$T_c$ superconductivity, spin electronics and more generally low-dimensional spin-driven systems, which are at the forefront of condensed matter physics. On the other, the thermal neutron is a highly penetrating, itinerant magnetic particle experiencing in parallel two force fields which are highly relevant in the discussion: the point scattering potential at nuclei position and the magnetic induction field associated with unpaired electron spins and trajectories. The resulting scattering amplitudes being of similar size and coherent in phase the neutron behavior is directly influenced by static and dynamic correlation existing between the positions of the nuclei and the behavior of the magnetic electrons.

Indeed, theory of inelastic neutron scattering has shown that the transverse component of scattered polarization is a direct signature of the existence of mixed nuclear-magnetic pair correlation functions [15]. Measurements are now being done systematically on several interesting systems showing that polarimetric neutron scattering effects are large and may well have a serious impact on the future understanding of microscopic physics in low-dimensional, spin driven systems. It seems that, in certain special situations, the magnetic moment of an atom depend significantly on its instantaneous position relative to the crystal or that some magnetic electrons are hoping periodically on various equivalent positions taking advantage of an underlying local lattice distortion. More theoretical work is needed to build appropriate models taking into account the fact that neutron has detected the hybrid nature of the excitation.

## Acknowledgements

The work described in this paper would not have been possible without the help of many colleagues and collaborators at ILL. We particularly acknowledge scientific collaboration with P.J. Brown, B. Forsyth, E. Lelièvre-Berna, L.P. Regnault, V. Nunez, T. Roberts, H. Humblot, J. Dreyer and technical collaboration with S. Pujol, E. Bourgeat-Lami, J. Allibon. The help of M. Thomas was decisive during the conception phase of Cryopad-II.

## References

[1] M. Blume, Phys. Rev. 130 (1963) 1670.
[2] S.V. Maleev, V.G. Bar'yakhtar, R.A. Suris, Fiz. Tv. Tela 4 (1962) 3461 [Sov. Phys. – Solid State, 4(12) (1963) 2533.]
[3] R.M. Moon, T. Riste, W. Koehler, Phys. Rev. 181 (1969) 920.
[4] H. Alperin, in: International Conference on Magnetism, 1973, Moscow, Proc. ICM-73.
[5] M.T. Rekveldt, J. Phys. (France) Coll. C1 (1971) 579.
[6] A.I. Okorokov, V.V. Runov, A.G. Gukasov, Nucl. Instrum. Meth. A 157 (1978) 487.
[7] F. Tasset, Physica B 156–157 (1989) 627.
[8] P.J. Brown, J.B. Forsyth, F. Tasset, Proc. R. Soc. Lond. A 442 (1993) 147.
[9] F. Tasset et al., Physica B 267–268 (1999) 69.
[10] F. Tasset et al., Physica B 241–243 (1998) 177.
[11] P.J. Brown et al., ILL Annual Report, 1999, Grenoble, pp. 52–53.
[12] P.J. Brown et al., Physica B 267–268 (1999) 215.
[13] W. Heil et al., Physica B 267–268 (1999) 328.
[14] L.P. Regnault et al., Physica B 267–268 (1999) 227.
[15] S.V. Maleyev, Physica B 267–268 (1999) 236.
[16] G.M. Drabkin et al., Sov. Phys. JETP 20 (1965) 1548.